ANALYSIS OF STRUCTURE, MICROSTRUCTURE AND CHEMICAL COMPOSITION OF SOLID SOLUTION OF CO-DOPED BARIUM CALCIUM STANNATE TITANATE (BA$_{1-X}$CA$_X$TI$_{0.975}$SN$_{0.025}$O$_3$) (0 ≤ X ≥ 0.12)

U. Ahmadu, M.I. Abdullahi, Abdulwaliyu B. Usman, Uno, E. Uno. and Moses Agida

Department of Physics, Federal University of Technology, P.M.B., 65, Minna, Nigeria

Corresponding author: u.ahmadu@ yahoo.com

Abstract

Ba$_{1-x}$Ca$_x$(Ti$_{0.975}$Sn$_{0.025}$)O$_3$ (0.00 $\leq$ x $\leq$ 0.12) ceramics have been synthesized by solid state reaction method. Structural analyses have been carried out to determine the effect of Ca^{2+} substitution on the structural parameters of the ceramic. The average crystallite size decreased from 36.39 nm to 35.39 nm for highly doped Ca^{2+}. Highest increase in c/a ratio was observed at x = 0.06. Microstructural evaluation of the material revealed decrease in grain size from 1 μm to 0.45 μm upon incorporation of Ca^{2+}. Energy Dispersive Spectroscopy (EDS) investigation showed variation in chemical composition but no structural transformation was observed.

Keywords: ceramic; X-ray diffraction; crystallinity; microstructure; grain size.

1. Introduction

Lead based perovskite ceramics have shown high dielectric and piezoelectric properties which are widely used in piezoelectric devices (Mahajan et al, 2011). Unfortunately, the lead content in such ceramics is a very toxic substance that can pollute environment, cause damage to brain and nervous system (Shi *et al*, 2013), hence from environmental point of view and human health protection, there is need to replace these materials with lead-free composition. Over the years, there have been growing researches in developing lead-free piezoelectric materials which may replace their lead-based counterparts. Perovskite Barium Titanate (BaTiO$_3$ or BT) has been recognized as a promising candidate due to its potential application in multilayer ceramic capacitors, piezoelectric transducers, sensors, Fe-RAM (Medhi and Nath, 2013), among others. BT is a typical ferroelectric which exhibits a perovskite (ABO$_3$) structure. However, some of its drawbacks have limited its extensive application in its pure form due to conflict between significant hysteresis in the strain and electric field dependence of the material which has led to difficulties in controlling the piezoelectric ceramic (Medhi and Nath, 2013), alongside its low piezoelectric constant (Aksel and Jones, 2010). Thermal instability of its structural phase and other dependent properties is also of major concern. BT exhibits a relatively low transition temperature (T_c=120 °C) and thus suffers structural phase transformation (ferroelectric-tetragonal to paraelectric-cubic phase) at low temperatures (Frattini *et al*, 2012; Aksel and Jones, 2010). Several attempts at improving its structural stability and other dependent properties such as ferroelectric and dielectric properties have been made (Dash *et al*, 2014; Kumar *et al*, 2009 and Woodecka-Duš *et al*, 2007). These include the substitution of Ba^{2+} or Ti^{4+} by atoms of different sizes and oxidation states resulting in compounds of different physical and chemical properties, while still retaining the same structural phase (Dash *et al*, 2014; Cai *et al*, 2011 and Kumar *et al*, 2009). It has been reported that partial substitution of Ba^{2+} by Ca^{2+} prevents grain growth, improves electromechanical properties and structural stability (Matsura *et al*, 2014;Choi *et al*, 2010 and Paunovic *et al*, 2004). However, it was observed that the substitution decreased the dielectric constant (Choi et al, 2010; Yun *et al*, 2007). But the substitution of Ti^{4+} by 0.025 mol of Sn^{4+} leads to increased permittivity, enhanced piezoelectric properties and decreased T_c [(Nath and Medhi, 2012). As such, it is expected that simultaneous substitutions of Ba^{2+} by Ca^{2+} and Ti^{4+} by Sn^{4+} (0.025 mol) may offer the possibility of developing a lead free piezoelectric ceramic. However, secondary phases which affect the crystal structure and other dependent properties of BT upon substitution of inappropriate Ca^{2+} concentration have been reported (Choi *et al*, 2010). Therefore, the appropriate concentration of Ca^{2+} that may improve the structural phase of the ceramic is worth

investigating. To the best of our knowledge, structural and microstructural properties of BT partially substituted by Ca^{2+} and Sn^{4+} (0.025 mol) have not been investigated apart from our earlier work (Ahmadu *et al*, 2016). In the present work, the effect of Ca^{2+} substitution (on the Ba^{2+} site of $BaTiO_3$) on the structural and microstructural properties of $Ba_{1-x}Ca_x(Ti_{0.975}Sn_{0.025})O_3$ ceramics (where, $0.00 \leq x \leq 0.12$) has been investigated and the evolution of these properties with doping have been reported.

2. Experimental Procedures

$Ba_{1-x}Ca_x(Ti_{0.975}Sn_{0.025})O_3$ (BCST) ceramics where $0.00 \leq x \leq 0.12$ were synthesized by solid state reaction method. Analytical grade $BaCO_3$ ($\geq 99\%$, Kermel, China.), TiO_2 and $CaCO_3$ (99.9%, Qualikems, India) and SnO_2 (99.99 %, BDH, U.K) were used as starting precursors. Stoichiometric amounts of these materials for the required specimens were weighed and dry- mixed thoroughly followed by wet mixing with distilled water as the medium. The amount of distilled water used was just enough to form slurry to prevent selective sedimentation of the reagents. The slurry was dried in an oven at 150 °C for 1 hour. The dried mixture was hand- ground thoroughly for homogeneity using agate mortar and pestle for 4 hours. The homogenous mixture was placed in an alumina crucible and calcined at 1050 °C for 4 hours in a furnace to allow volatilization of bye-product, CO_2. The obtained mixed powder was further ground for 1 hour and granulated by adding 4 wt% polyvinyl alcohol (PVA) as binder to reduce brittleness and to have better compactness and then pressed into 26 mm diameter and 1 mm thickness pellets at a pressure of 10 tons. Finally, the prepared pellets were sintered at 1100 °C for 3 hours, and furnace-cooled to obtain a crystal phase formation.

X-ray Diffractometer (D8 Advance, BRUKER AXS, 40 kV, 40 mA) with monochromatic $Cu-K_{\alpha}$ radiation (λ = 1.54060 Å) at iThemba LABs, South Africa, was used to characterize the structural phase composition of the synthesized ceramics over a 2θ range from 20° to 90° with scan step and acquisition time of 0.034° and 88 seconds, respectively. The morphology and the elemental composition of the ceramics were analyzed using High Resolution Scanning Electron Microscope (HRSEM, Zeiss) coupled with EDS spectrometer, working at a voltage of 20 kV at the Electron Microscopy Unit, Department of Physics at the University of the Western Cape (UWC), Cape Town, South Africa. Images were captured at 5 kV. Prior to the analysis, the samples were placed on a carbon adhesive tape and backed on an aluminium stage. As the samples are non-conducting, a thin layer of AuPd was coated using a sputter coater and then vacuumed in the HRSEM. For measurement of the grain sizes, Imagej software was used.

3. Results and Discussion

3.1 Crystal Structure Analysis

X-ray Diffraction (XRD) patterns of the synthesized $Ba_{1-x}Ca_x(Ti_{0.975}Sn_{0.025})O_3$ ceramics, with x = 0.00, 0.06 and 0.12 mol is depicted in Fig. 1.The XRD patterns confirm that the ceramics are polycrystalline with single phase perovskite structure which compares well with JCPDS no: 00-005-0626 reference data of tetragonal $BaTiO_3$. The XRD patterns are also in agreement with the reports of other workers who prepared BT-based ceramics using similar method (Kim *et al*, 2009;Fasasi *et al*, 2006).
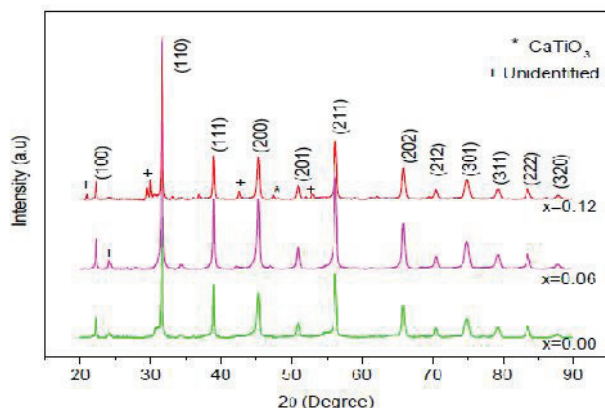
Figure 1. X-Ray Diffraction Pattern of $Ba_{1-x}Ca_x(Ti_{0.975}Sn_{0.025})O_3$ $(0.00 \leq x \leq 0.12)$

However, a minor peak around 47.5° 2θ scan was observed at x = 0.12 which has been identified as orthorhombic $CaTiO_3$ phase (JCPDS file no: 00-022-0153) and attributed to the solubility limit of Ca^{2+} in BCST. This suggests that Ca^{2+} is soluble in BCST up to 0.06 mol. There were other diffraction peaks though with very low intensities whose match could not be found as indicated in the XRD spectra. Further, it was observed that the structure sensitive peak (200) slightly shift towards higher 2θ angles from 45.246 to 45.261° with increasing Ca^{2+} concentration. This suggests distortion of the ABO_3 unit cell lattice (Chen and Yuan-fang, 2012) which could lead to changes in the lattice parameters and is consistent with fact that the radius of Ca^{2+} ions (0.99 Å) is smaller than that of Ba^{2+} ions (1.34 Å) (Yun et al, 2007).

Average crystallite size (s) were calculated by eqn. (1) (Dash et al, 2014) using the full width at half maximum (FWHM) of the most intense peak.

$$D = \frac{0.9\lambda}{\beta \cos \theta} \qquad (1)$$

where β is the FWHM of the diffraction peak expressed in radians, θ is the Bragg diffraction angle of the XRD peak, λ is the wavelength of the X-ray used which is 1.54060 Å and D is the crystallite size in nanometers.

The calculated average crystallite size is presented in table 1 where it can be seen that the crystallite size decreased because FWHMs increased with increase in doping concentration. This is due to the fact that smaller Ca^{2+} ions replace larger Ba^{2+} ions and their reactivity with the host compound decreased giving rise to decreased crystallinity.

Table 1: Ca^{2+} Concentration (x), Peak Position (2θ) and FWHM (β) at (110) and Average Crystallite size (D)

x	2θ (Degree)	$\beta \times 10^{-3}$ (Radians)	D (nm)
0.00	31.57	3.61	36.93
0.06	31.59	3.94	33.82
0.12	31.58	3.77	35.39

Lattice parameters *a* and *c* of the ceramics were calculated from the XRD spectra using the (100), (200) and (201) diffraction peaks and compared with the JCPDS no: 00-005-0626 data of BaTiO$_3$ (table 2).

Table 2: Determined Lattice Constants a and c, c/a and Cell Volume of Ba$_{1-x}$Ca$_x$(Ti$_{0.975}$Sn$_{0.025}$)O$_3$ Ceramics

X	a (Å)	c (Å)	c/a (Å)	Cell Volume (Å^3)
Referenced BT	3.994	4.038	1.0110	64.410
0.00	4.0048	4.0092	1.0011	64.30
0.06	4.0030	4.0149	1.0030	64.30
0.12	4.0020	4.0110	1.0022	64.20

It can be seen that x = 0.00 is weakly tetragonal in comparison with the JCPDS data of BaTiO$_3$ prepared at higher temperature. But on substitution of Ca^{2+} for Ba^{2+}, the lattice parameters *a* decreased while *c* increased and consequently *c/a* ratio (tetragonality) increased. However, x = 0.06 is seen to have the highest value, which could be attributed to the solubility limit of Ca^{2+}. It has been suggested that the increase of the space available to the Ca^{2+} at the Ba^{2+} site induced ferroelectricity in dielectrics (Choi *et al*, 2010). It is hypothesized this could be the reason for the increase in tetragonality observed on substitution of Ba^{2+} by Ca^{2+}. Also presented in table 2 is the cell volume where it is seen to slightly decrease as the concentration of Ca^{2+} increased. This has been corroborated by shifting of (200) peaks to higher angles with increasing Ca^{2+} concentration. Moreover, increase in *c/a* is a desirable characteristic of perovskite titanates because higher *c/a* normally increases the polarizability and improves the ferroelectric properties (Mady, 2011). Thus the observed increase in tetragonality of Ba$_{1-x}$Ca$_x$(Ti$_{0.975}$Sn$_{0.025}$)O$_3$ (0.00 $\leq$ x $\leq$ 0.12) may lead to improved ferroelectric properties. Thus it was found that the most appropriate structural properties of Ba$_{1-x}$Ca$_x$(Ti$_{0.975}$Sn$_{0.025}$)O$_3$ ceramics can be obtained with x = 0.06.

3.2 Microstructural Analysis
Fig. 2 depicts HRSEM micrographs of Ba$_{1-x}$Ca$_x$(Ti$_{0.975}$Sn$_{0.025}$)O$_3$ (0.00 $\leq$ x $\leq$ 0.12). From Fig. 2(a), it can be seen that the particles agglomerate alongside fairly homogeneous and porous microstructure.
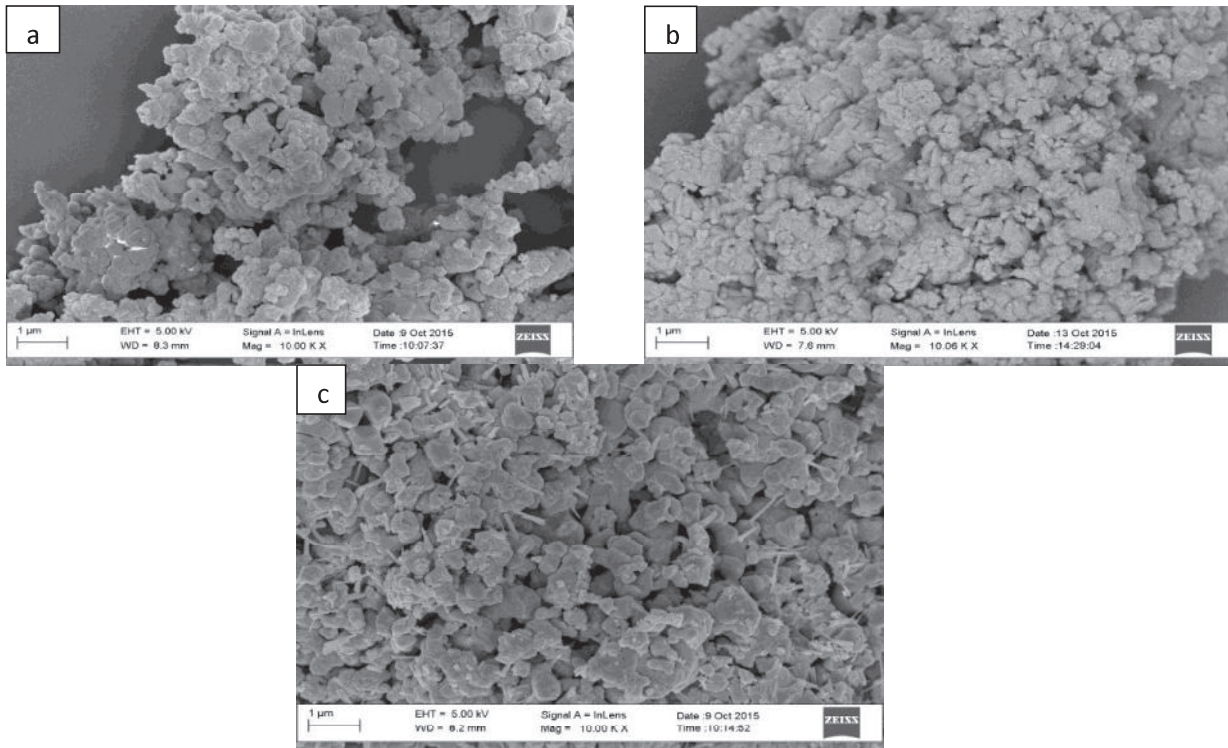
Figure2. HRSEM Micrographs of (a) x = 0.00 (b) x = 0.06 (c) x = 0.12

The average grain size of the ceramics is about 1 μm which is smaller than those observed in traditional BT ceramics sintered at higher temperature (1450 °C) (Nath and Medhi, 2014). The small value of grain size may be due to insufficient sintering temperature. On addition of Ca^{2+} (x = 0.06), harder agglomeration of grains is observed and the average grain size decreased to about 0.45 μm and this eventually gives rise to poor microstructure (Figure 2b). As Ca^{2+} concentration increased (x = 0.12), two regions are distinguishable in their grain size and phase compositions. The first shows a fairly fine-grained microstructure with average grain size of 0.7 μm , while the other has rod-like grains (Figure 2c). Some residual porosity is evident. The distinct feature of this sample is the presence of non-homogeneous microstructure throughout the sample. The observed rod-like grains are due to non-uniform distribution of starting powders (Paunovic *et al.,* 2004). It is generally known that the initial powder preparation process and possibly insufficient mixing of starting powders or insufficient sintering temperature could result in poor and non-homogeneous microstructure. The decrease in average grain size of the ceramic upon substitution of Ca^{2+} for Ba^{2+} indicates that Ca^{2+} inhibits grain growth (Choi *et al.*, 2010). Moreover, ferroelectric properties of BT-based ceramics have been strongly linked to grain size (Nath and Medhi, 2014) where it is found to decrease when grain size decreases. Decrease in dielectric constant may also be expected because the grain boundary is non-ferroelectric and the dielectric constant of grain boundary is much less than that of grain (Cai *et al.,* 2011). The smaller the grain size is, the more the grain boundary is, and therefore the lower the dielectric constant is.

3.3 Chemical Composition

Fig. 3 is the EDS spectrum showing the elemental composition of $Ba_{1-x}Ca_x(Ti_{0.975}Sn_{0.025})O_3$ ceramics. All the peaks have been identified with the potential elements that match that peak. The spectra clearly reveal the presence of Ba,
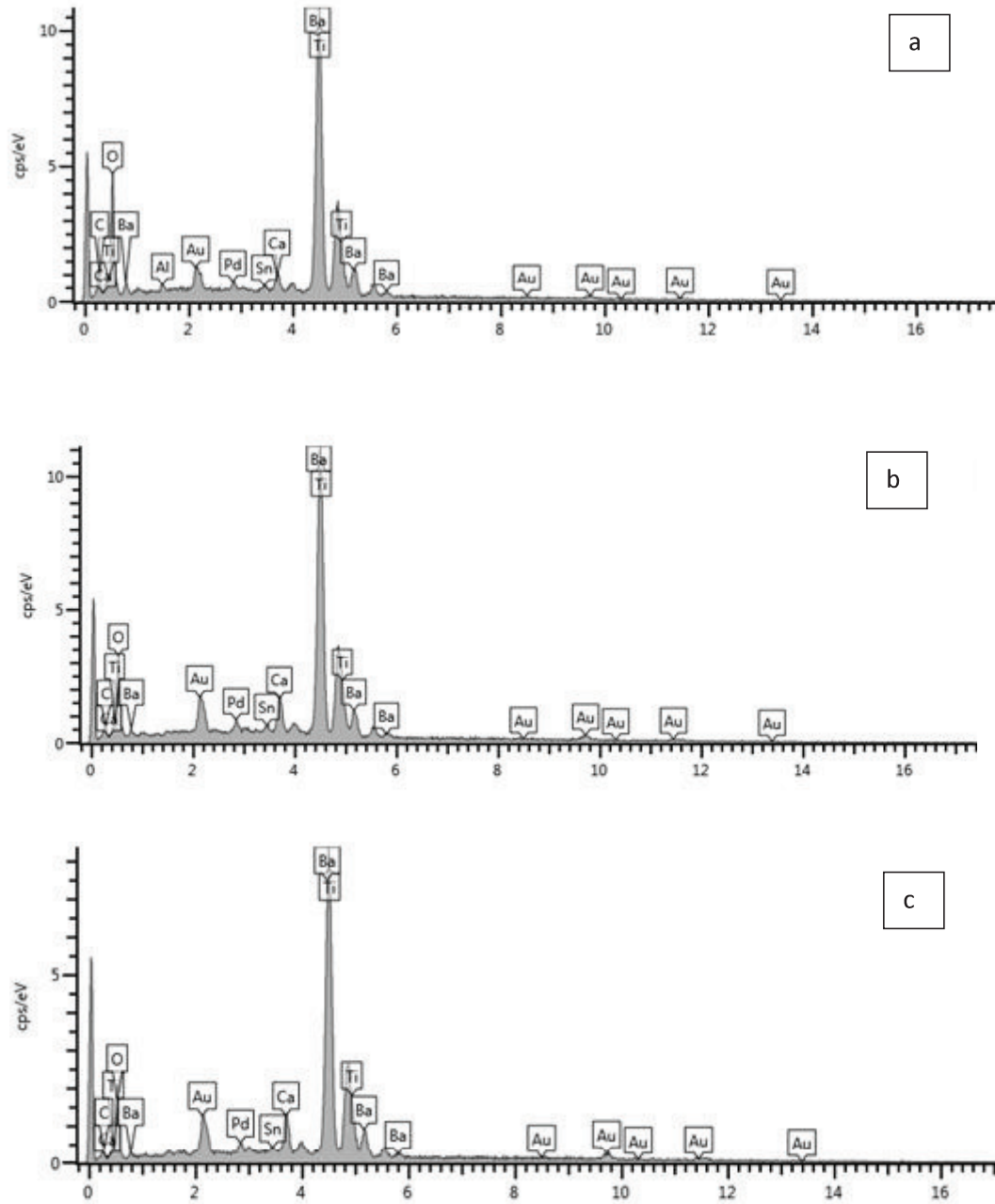

Fig. 3: EDS spectrum of (a) x = 0.00 (b) x = 0.06 (c) x = 0.12

The C (carbon) source could have come from the carbon tape. AuPd (Gold-Paladium) is present in the compound in order to make it conducting and the Al may be attributed to contamination during the preparation of samples for SEM analysis. Table 3 gives a quantitative comparison of the nominal composition and the normalized EDS derived composition where the major sources of error have been removed and the remaining elements normalized to 100% to give a representation of the elements present in the compound. The variations in the normalized EDS

derived composition in comparison with the nominal composition could be assigned to deficiency of oxygen during sintering in the ambient (Bapanda, 2010). The overlap of Ba and Ti is clear in the spectra and makes it difficult to distinguish between them in the quantification results. This observation has been reported by other workers (Kim *et al*, 2009;Fasasi *et al*, 2006). However, further investigations are required to elucidate the higher values of the normalized EDS derived results.

Table 3.Nominal and Normalized EDS-derived Elemental Composition

Sample (x)	Nominal Composition (atomic %)						Normalized EDS Derived Composition (atomic %)					
	Ba	Ca	Sn	Ti	O	Total	Ba	Ca	Sn	Ti	O	Total
0.00	20.00	-	0.50	19.50	60.00	100	18.41	-	0.33	19.11	62.15	100
0.06	18.80	1.20	0.50	19.50	60.00	100	19.59	3.59	0.63	22.97	52.69	100
0.12	17.60	2.4	0.50	19.50	60.00	100	22.31	4.7	0.4	26.64	45.95	100

4. Conclusion

Polycrystalline $Ba_{1-x}Ca_x(Ti_{0.975}Sn_{0.025})O_3$ $(0.00 \leq x \leq 0.12)$ ceramics were prepared by solid state reaction method. The results indicate that the FWHM increased, crystallite size and grain size decreased as the concentration of Ca^{2+} increased, all of which lead to reduced crystallinity. Variations are observed in the lattice parameters which cause lattice distortion and consequently lead to increase in *c/a* ratio alongside slight contraction of unit cell volume. The changes in the structural and microstructural properties observed on substitution of Ca^{2+} for Ba^{2+} in BCST ceramic could lead to changes in the dielectric and other properties.

References

Ahmadu Umaru, Ahmad Abubakar Soje, Abdulwaliyu Bidemi, Muhammad Auwal Musa, Isah Kasim Uthman. (2016).Structural and Microstructural Study of Gamma Ray-Irradiated Co-doped Barium Titanate $(Ba_{0.98}Ca_{0.12}Ti_{0.975}Sn_{0.025}O_3)$.*Processing and Application of Ceramics*,10 (2):79-85.

Aksel, E. and Jones, J.L. (2010) Advances in Lead-Free Piezoelectric Materials for Sensors and Actuators. *Sensors*, **10**, 1935-1954.

Badapanda, T. (2010). Structural, Electrical and Optical Study of 'A' Site Deficient Heterovalent Ion Doped Barium Zirconium Titanate Perovskite. *Department of physics, National Institute of Technology.*Rourkela-769008.Orissa India, 6-58.

Cai, W., Fu, C.L., Gao, J.C. and Zhao, C.X. (2011) Dielectric Properties and Microstructure of Mg doped barium titanate ceramics. *Adances in Applied Ceramics*, **110**, 3, 181-185.

Chen, Z. and Yuan-fang, Q.U. (2012) Dielectric Properties and Phase Transitions of La_2O_3- and Sb_2O_3-Doped Barium Strontium Titanate Ceramics. *Transactions of Nonferrous Metals Society of China,* **22**, 2742−2748.-I

Choi, Y.k., Hoshina, T., Takeda, H. and Tsurumi, T. (2010) Effects of Ca and Zr Additions and Stoichiometry on the Electrical Properties of Barium Titanate-Based Ceramics. *Journal of the Ceramic Society of Japan,* **118**, 10, 881-886.

Dash, S.K., Kant, S., Danlai, B., Swain, M.D. and Swain, B.B. (2014) Characterization and Dielectric Properties of Barium Zirconium Titanate Prepared by Solid State Reaction and High Energy ball milling processes. *Indian Journal of Physics*, **88**, 2, 129-135.

Fasasi, A.Y., Balogun, F.A., Fasasi, M.K., Ogunyele, P.O., Mokobia, C.E. and Inyang, E.P. (2006) Thermoluminescence Properties of Barium Titanate Prepared by Solid-State Reaction*, Sensors and Actuators A,* **135**, , 598-604.

Frattini, A., Di Loreto, A., de Sanctis, O. and Benavidez, E. (2012) BCZT Ceramics Prepared from Activated Powders. *Procedia Material Science,* **1**, 359-365.
HSIANG, FU-SU YEN, YEN-HWEI

Kim, Y.J., Hyun, J.W., Kim, H.S., Lee, J.H., Yun, M.Y., Noh, S.J. and Ahn, Y.H. (2009) Microstructural Characterization and Dielectric Properties of Barium Titanate Solid Solutions with Donor Dopants. *Bulletin of the Korean Chemical Society,* **30**, 6, 1267-1273.

Kumar, Y., Mohiddon, A. Md., Srivastava, A. and Yadav, K.L. (2009) Effect of Ni Doping on Structural and Dielectric Properties of $BaTiO_3$. *Indian Journal of Engineering & Material Sciences*, **16**, 390-394.

Mady, H. A. (2011) XRD and Electric properties of lead barium Titanate Ferroelectric Ceramic. *Australian Journal of Basic and Applied Sciences,* **5**, 10, 1472-1477.

Mahajan, S., Thakur, O.P., Prakash, C. and Sreenivas, K. (2011) Effect of Zr on Dielectric, Ferroelectric and impedance properties of BaTiO3 ceramic. *Bulletin of Materials Science,* **34**, 7, 1483–1489.

Matsuura, K., Hoshina, T., Takeda, H., Sakabe, Y. and Tsurumi, T. (2014) Effects of Ca Substitution on Room Temperature Resistivity of Donor-Doped Barium Titanate Based PTCR Ceramics. *Journal of the Ceramic Society of Japan,* **122**, 6, 402-405.

Medhi, N. and Nath, A.K. (2013) Gamma ray Irradiation Effects on Ferroelectric and Piezoelectric Properties of Barium Titanate Ceramics. *Journal of Material Engineering and Performance*, **22**, 2716-2722.

Nath A.K. and Medhi, A. (2014) Effect of Gamma Ray Irradiation on the Piezoelectric and Ferroelectric Properties of Bismuth Doped Barium Titanate Ceramics. *Indian Journal of Physics,* Doi: 10.1007/s12648-014-0531-5.

Nath, A.K. and Medhi, N. (2012) Density Variation and Piezoelectric Properties of $Ba(Ti_{1-x}Sn_x)O_3$ Ceramics Prepared from Nanocrystalline Powders. *Bulletin of Materials Science*, **35**, 5, 847–852.

Paunovic, V., Zivkocic, Z., Vracar, L., Mitic, V. and Miljkovic, M. (2004) The effect of additive on Microstructural and Electrical Properties of $BaTiO_3$. *Serbian Journal of Electrical Engineering,* **1**, 3, 89-98.

Shi, M., Zhong, J., Zuo, R., Xu, Y., Wang, L., Su, H. and Gu, C. (2013) Effect of Annealing Processes on the Structural and Electrical Properties of the Lead-Free Thin Films of $(Ba_{0.9}Ca_{0.1})(Ti_{0.9}Zr_{0.1})O_3$. *Journal of Alloys and Compounds*, **562**, 116–122.

Wodecka-Duś, B., Lisińska-Czekaj, A., Orkisz, T., Adamczyk, M., Osińska, K., Kozielski, L. and Czekaj, D. (2007) The Sol-gel Synthesis of Barium Strontium Titanate. *Materials Science-Poland,* **25**, 3, 719-799.

Yun, S., Wang, X., Li, B. and Xu, D. (2007) Dielectric Properties of Ca-Substituted Barium strontium Titanate Ferroelectric Ceramics. *Solid State Communications,* **143**, 461–465.